BULETINUL ACADEMIEI DE ŞTIINŢE
A REPUBLICII MOLDOVA. MATEMATICA
Number 3(46), 2004, Pages 91–109
ISSN 1024–7696

Modeling and optimization of melting and solidification process

A.F. Albou, V.I. Zubov

Abstract. An optimal control problem is considered for two-phase Stefan problem describing the process of melting and solidification. The problem is solved numerically by variation and finite-difference methods. The results are described and analyzed in detail. Some of them are presented as tables and plots.

Mathematics subject classification: 49J20, 93C20.
Keywords and phrases: Optimal control, melting and solidification process, Stephan problem, gradient.

1 Introduction

Heat transfer in various media has a great effect on many practically important processes. For this reason, many studies in both physics and mathematics have been devoted to this subject. Mathematically, heat transfer is described by boundary value problems for a heat equation. These boundary value problems have been thoroughly described and investigated in both handbooks and specialized literature.

Since few boundary value problems for the heat equation have analytical solutions, much effort has been focused on the development of numerical methods for problems of this kind.

Practically interesting problems concern not only the description and analysis of heat transfer processes but also the optimal control of them. As a result, the theory of optimal control of thermal processes has been created, which includes the existence and uniqueness of optimal solution, finite-difference approximation and regularization of optimal control problems, and solutions to specific practically important problems. Relevant results in this direction can be found, for example, in [1, 4].

An important class of heat transfer problems is that describing processes in which the substance under study undergoes phase changes accompanied by heat release or absorption. Problems of this kind (known as Stefan problems) arise in many situations, of which the most important and widespread are melting and solidification processes. An important feature of these problems is that they involve a moving interface between two phases (liquid and solid). The law of motion of the interface is unknown in advance and is to be determined. It is on this interface that heat release or absorption associated with phase changes occurs. The thermal properties of the substance on the different sides of the moving interface can be different. Problems of

© A. F. Albou, V. I. Zubov, 2004

this class are noticeably more complicated than those not involving phase changes. An analysis of direct Stefan problems and methods for their solution are broadly presented in scientific literature.

Studies concerning optimal control of processes with phase changes are relatively few. Interesting and important (in our view) studies in this area can be found in [5,6].

In this paper, we consider the following optimal control problem for the process of melting and solidification. Given a heat source with a time-varying strength (which is treated as a control function), the problem is to find a source strength temporal distribution such that no less than a prescribed portion of the sample is melted, solidification proceeds at a rate not exceeding a prescribed magnitude, and the total heat supplied by the source is minimal.

This problem is analyzed here in a one-dimensional (radially symmetric) time-dependent setting. The heat source is located along the axis of symmetry. We analyze the case of a distributed and a point source. The control function is subject to inequality constrains, which simulate requirements imposed on the process of melting and solidification.

2 The mathematical formulation of the problem

In the plane of independent variables (r,t) we consider a rectangular domain $Q = \{(r,t) : 0 < r < R, 0 < t \le \Theta\}$ (see Fig. 1). a smooth curve AB with the equation $r = \xi(t)$ divides Q into two subdomains: L (liquid domain) and S (solid domain). The curve AB is the trajectory of the front of melting and solidification. Let $t_0 \ge 0$ be the time at which AB originates. Then L and S are defined by

$$L = \{(r,t) : \quad 0 < r < \xi(t), \quad t_0 < t \le \Theta\},$$

$$S = \{(r,t) : \quad \xi(t) < r < R, \quad 0 < t \le \Theta\}.$$

In Q we consider the two-phase Stefan problem

$$M_L \equiv \rho_L C_L \frac{\partial T_L}{\partial t} - \frac{1}{r}\frac{\partial}{\partial r}\left(r k_L \frac{\partial T_L}{\partial r}\right) - F(r,t) = 0, \qquad (r,t) \in L, \tag{1}$$

$$M_S \equiv \rho_S C_S \frac{\partial T_S}{\partial t} - \frac{1}{r}\frac{\partial}{\partial r}\left(r k_S \frac{\partial T_S}{\partial r}\right) - F(r,t) = 0, \qquad (r,t) \in S, \tag{2}$$

$$T_S(r,0) = T_{in}(r), \qquad 0 < r < R, \tag{3}$$

$$T_L\left(\xi(t),t\right) = T_S\left(\xi(t),t\right) = T_{pl}, \qquad t_0 \le t \le \Theta, \tag{4}$$

$$\left[k_S \frac{\partial T_S}{\partial r}\right]\Bigg|_{(\xi(t)+0,t)} - \left[k_L \frac{\partial T_L}{\partial r}\right]\Bigg|_{(\xi(t)-0,t)} = \rho_S \lambda \xi'(t), \qquad t_0 \le t \le \Theta, \tag{5}$$

$$k_S \frac{\partial T_S}{\partial r}\Bigg|_R = \alpha\left[T_{ex} - T_S(R,t)\right], \qquad 0 < t \le \Theta, \tag{6}$$

$$\frac{\partial T_L}{\partial r}(0,t) = 0, \qquad t_0 < t \le \Theta, \tag{7}$$

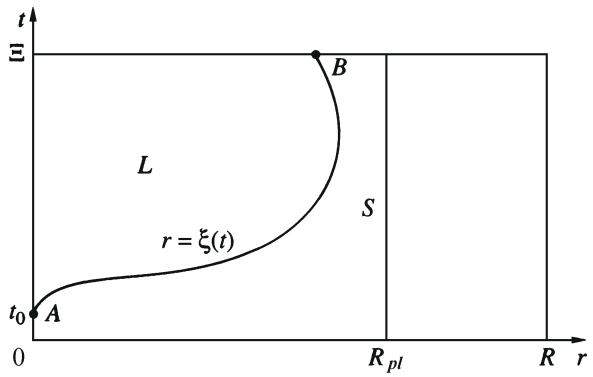

Fig. 1

$$\frac{\partial T_S}{\partial r}(0,t) = 0, \qquad 0 < t < t_0. \tag{8}$$

Here, $T(r,t)$ is the substance temperature at the point with coordinates (r,t); ρ, C, and k are the substance density, specific heat capacity, and thermal conductivity, respectively; λ is the heat of fusion of the substance; the subscripts L and S denote the liquid and solid phases, respectively; T_{pl} is the temperature of fusion; $T_{in}(r)$ is the initial temperature of the substance, $T_{in}(r) \le T_{pl}$; α is the heat exchange coefficient with the surrounding medium; and T_{ex} is the ambient temperature.

The source $F(r,t)$ of input heat can be represented as $F(r,t) = \varphi(r)f(t)$, where $\varphi(r)$ is a given function describing the spatial distribution of supplied heat. Along with $\varphi(r)$ and $f(t)$, the source of input heat will also be characterized by the function

$$f_w(t) = \int_0^\infty 2\pi r F(r,t)dr = f(t)\int_0^\infty 2\pi r\varphi(r)dr.$$

Especially worth noting is the particular case where $\varphi(r) = \delta(r)$ is the delta function (a point source). Overall, the statement of direct problem (1)—(8) then remains the same, except that we set $F(r,t) \equiv 0$ and $t_0 = 0$ in Eqs. (1), (2) and conditions (7) and (8) are replaced by

$$\lim_{r\to 0}\left(-2\pi k_L r\frac{\partial T_L}{\partial r}\right) = f(t), \qquad 0 < t \le \Theta. \tag{9}$$

Note that $f(t)$ coincides with $f_w(t)$ for a point source.

Problem (1)—(8) (or (1)—(6), (9)) with a given $f(t)$ is referred to as the direct problem.

Let $\xi(t)$ be the interface corresponding to the source $f(t)$, $t \in [0,\Theta]$, and let ξ_f be the maximum of $\xi(t)$ over $t_0 \le t \le \Theta$. The function $f(t)$ is said to belong to $K(\Theta)$ if it satisfies the following conditions:

(i) it is defined and piecewise continuous on $[0,\Theta]$;

(ii) it has a piecewise continuous derivative;

(iii) it satisfies $0 \le f(t) \le f_{max}$ for all $t \in [0, \Theta]$;
(iv) the corresponding $\xi_f \ge R_{pl}$, where R_{pl} is given and satisfies $R_{pl} < R$;
(v) it holds that for all $t \in [0, \Theta - \beta^2]$

$$\xi^{'}(t) \ge -d^2. \tag{10}$$

Note that the value of f_{max} can be infinitely large, i.e., unbounded from above. Note also that, for a given finite f_{max}, Θ cannot be less than a certain value, because otherwise the class $K(\Theta)$ will be empty.

The variation problem to be solved is stated as follows: among the functions $f(t)$ in $K(\Theta)$, find $f_{opt}(t)$ that minimizes the functional

$$J = \int_0^{\Theta} f(t)dt. \tag{11}$$

The objective functional J is proportional to the total heat J_w supplied by the source over the observation time and equal to

$$J_w = \int_0^{\Theta} f_w(t)dt. \tag{12}$$

For mathematical modeling of the direct problem (determination of temperature distribution and interface separating the phases when control function – supplied heat – is given) the numerical algorithm was worked out and realized.

3 The algorithm of solving the direct problem

The algorithm that solves the direct problem is designed to deal with a distributed source, when $\varphi(r) \ne \delta(r)$. Essentially, it is a non front-capturing algorithm. The main idea of the algorithm was proposed by M. Rose in [7] and was developed by R.E. White in [8,9]. Here the path of the interface is not regarded as an explicitly imposed interior boundary condition. M.E.Rose suggested a generalized formulation of the problem and shows that genuine solution of the problem is its weak solution. On the other hand two genuine solutions whose domains of definition are separated by a smooth curve will constitute a weak solution if and only if the Stefan conditions (4), (5) connecting solid and liquid phases on the line take place.

In accordance with [7] we change from the unknown temperature $T(r,t)$ to the enthalpy function $E(r,t)$ defined in terms of temperature as

$$E(T) = \begin{cases} \rho_S C_S T, & T < T_{pl}, \\ \rho_L C_L (T - T_{pl}) + \rho_S C_S T_{pl} + \rho_S \lambda, & T \ge T_{pl}. \end{cases}$$

Note that the function $E(T)$ has a jump at the melting point T_{pl}. Treating the enthalpy $E(r,t)$ as a basic variable and the temperature $T(E)$ as defined by the

relation

$$T(E)=\begin{cases} E\rho_S^{-1}C_S^{-1}, & E<E_-=\rho_S C_S T_{pl},\\ T_{pl}, & E_-\le E\le E_+=E_-+\rho_S\lambda,\\ \left[E+(\rho_L C_L-\rho_S C_S)T_{pl}-\rho_S\lambda\right]\rho_L^{-1}C_L^{-1}, & E_+<E \end{cases}$$

one can consider temperature as a continuous function of enthalpy.

In the general case, the heat conductivity depends on temperature and has a jump at the melting point, which corresponds to a transition from solid to liquid phase. In the proposed algorithm, the heat conductivity is a function of enthalpy defined as

$$\Omega(E)=k(T(E))=\begin{cases} k_S, & E<E_-,\\ k_S+(E-E_-)(k_L-k_S)(E_+-E_-)^{-1}, & E_-\le E\le E_+,\\ k_L, & E>E_+. \end{cases}$$

Problem (1)–(8) is reformulated in terms of the enthalpy function $E(r,t)$ as

$$\begin{aligned} &\frac{\partial E}{\partial t}=\frac{1}{r}\frac{\partial}{\partial r}\left(r\Omega(E)\frac{\partial T(E)}{\partial r}\right)+F(r,t), && (r,t)\in Q,\\ &E(r,0)=E(T_{in}(r)), && 0<r<R,\\ &\left.\frac{\partial E}{\partial r}\right|_{r=0}=0, && 0\le t\le\Theta,\\ &\Omega(E)\left.\frac{\partial T(E)}{\partial r}\right|_{r=R}=\alpha\left[T_{ex}-T(E(R,t))\right], && 0\le t\le\Theta. \end{aligned} \tag{13}$$

To approximate the boundary value problem (13) in the domain Q, we introduce a nonuniform grid $\omega=\{r_i,t^j\}$, where

$$r_0=t^0=0,\ \ r_i=r_{i-1}+h_{i-1},\ \ t^j=t^{j-1}+\tau^j,\ \ (i=1,\dots,K;j=1,\dots,M).$$

Using an implicit approximation with respect to time and an integro-interpolation method, we obtain the following system of finite-difference equations:

$$\begin{aligned} &E_0^j+a_0\hat\Omega(E_0^j)T(E_0^j)-a_0\hat\Omega(E_0^j)T(E_1^j)=E_0^{j-1}+\tau^jF_0^j,\\ &E_i^j+[a_i\hat\Omega(E_i^j)+b_i\hat\Omega(E_{i-1}^j)]T(E_i^j)-b_i\hat\Omega(E_{i-1}^j)T(E_{i-1}^j)-\\ &-a_i\hat\Omega(E_i^j)T(E_{i+1}^j)=E_i^{j-1}+\tau^jF_i^j, \qquad (1\le i\le K-1),\\ &E_K^j+[a_K\alpha+b_K\hat\Omega(E_{K-1}^j)]T(E_K^j)-b_K\hat\Omega(E_{K-1}^j)T(E_{K-1}^j)=\\ &=a_K\alpha T_{ex}+E_K^{j-1}+\tau^jF_K^j,\\ &\qquad j=1,\dots,M. \end{aligned} \tag{14}$$

Here, we introduce the following notation:

$$a_0 = \frac{4\tau^j}{h_0^2}, \qquad a_K = \frac{8\tau^j r_K}{4r_K h_{K-1}(1-h_{K-1})}, \qquad b_K = \frac{4\tau^j(2r_k - h_{K-1})}{h_{K-1}^2(4r_k - h_{K-1})},$$

$$a_i = \frac{4\tau^j(2r_i + h_i)}{4r_i h_i(h_i + h_{i-1}) + h_i^3 - h_{i-1}^2 h_i}, \quad b_i = \frac{4\tau^j(2r_i - h_{i-1})}{4r_i h_{i-1}(h_i + h_{i-1}) - h_{i-1}^3 + h_i^2 h_{i-1}},$$

$$(i = 1, \ldots, K-1),$$

$$E_i^j = E(r_i, t^j), \qquad F_i^j = F(r_i, t^j), \qquad \hat{\Omega}(E_i^j) = \Omega[(E_i^j + E_{i+1}^j)/2].$$

The system of finite-difference equations (14) is an implicit approximation of the boundary value problem (13) restricted to $O(\tau, h^2)$ terms, where $\tau = \max\limits_j \tau^j$, $h = \max\limits_i h_i$.

The system of algebraic equations (14) can be split into M subsystems relating the enthalpy dependent quantities calculated on the j-th time layer with those calculated on the $(j-1)$-th time layer, $j = 1, \ldots, M$. To facilitate further analysis, we represent the dependence of temperature T on E as $T(E) = \mu E + \nu$, where the functions μ and ν are defined as follows:

$$\mu(E) = \begin{cases} \rho_S^{-1} C_S^{-1}, & E < E_-, \\ 0, & E_- \le E \le E_+, \\ \rho_L^{-1} C_L^{-1}, & E_+ < E, \end{cases}$$

$$\nu(E) = \begin{cases} 0, & E < E_-, \\ T_{pl}, & E_- \le E \le E_+, \\ \left((\rho_L C_L - \rho_S C_S) T_{pl} - \rho_S \lambda\right) \rho_L^{-1} C_L^{-1}, & E_+ < E. \end{cases}$$

We also introduce $(K+1)$-dimensional vectors $\mathbf{D}(\mathbf{E}^j)$, $\mathbf{L}(\mathbf{E}^j)$, $\mathbf{U}(\mathbf{E}^j)$ and $\boldsymbol{\eta}^j$, defined in terms of the components of the $(K+1)$-dimensional vector $\mathbf{E}^j = \|E_0^j\ E_1^j \ldots E_K^j\|^T$ by the relations

$$\begin{aligned}
&D_0(\mathbf{E}^j) = a_0 \hat{\Omega}(E_0^j), \quad D_K(\mathbf{E}^j) = \alpha a_K + b_K \hat{\Omega}(E_{K-1}^j), \\
&D_i(\mathbf{E}^j) = a_i \hat{\Omega}(E_i^j) + b_i \hat{\Omega}(E_{i-1}^j), && (i = 1, \ldots, K-1), \\
&L_0(\mathbf{E}^j) = 0, \qquad L_i(\mathbf{E}^j) = b_i \hat{\Omega}(E_{i-1}^j), && (i = 1, \ldots, K), \\
&U_K(\mathbf{E}^j) = 0, \qquad U_i(\mathbf{E}^j) = a_i \hat{\Omega}(E_i^j), && (i = 0, \ldots, K-1), \\
&\eta_K^j = a_K \alpha T_{ex} + E_K^{j-1} + \tau^j F_K^j, \qquad \eta_i^j = E_i^{j-1} + \tau^j F_i^j, && (i = 0, \ldots, K-1).
\end{aligned}$$

Now, the j-th subsystem of (14) $(j = 1, \ldots, M)$ can be written as

$$E_i^j + D_i(\mathbf{E}^j) T(E_i^j) - L_i(\mathbf{E}^j) T(E_{i-1}^j) - U_i(\mathbf{E}^j) T(E_{i+1}^j) = \eta_i^j, \tag{15}$$

$$(i = 0, \ldots, K).$$

In [8], two iterative algorithms were proposed for solving the nonlinear system of equations (15). One of them is based on a modified Jacobi method. Defining the

$(K+1)$-dimensional vector $\mathbf{V}^n = \|V_0^n\ V_1^n \dots V_K^n\|^T$ obtained as the approximation of $\mathbf{E}^j$ at the n-th iteration step (the initial approximation $\mathbf{V}^0$ is the vector $\mathbf{E}$ calculated on the preceding time layer, i.e., $\mathbf{E}^{j-1}$), we formulate the modified Jacobi method as the iterative calculation of the vector $\mathbf{V}^{n+1}$ given by the relation

$$V_i^{n+1}=(1-\omega)V_i^n+\omega\frac{L_i(\mathbf{V}^n)T(V_{i-1}^n)+U_i(\mathbf{V}^n)T(V_{i+1}^n)-D_i(\mathbf{V}^n)\nu(V_i^n)+\eta_i^j}{1+D_i(\mathbf{V}^n)\mu(V_i^n)}, \qquad (16)$$

$$(i=0,\dots,K).$$

The iteration is continued until the relative difference in the values of the desired function between consecutive iteration steps,

$$\varepsilon = \max_{i=0,\dots,K}\frac{V_i^{n+1}-V_i^n}{V_i^n}$$

(i.e., the iteration error), becomes less than a required value.

The other algorithm proposed in [8] is based on a modified Gauss-Seidel method. In this algorithm, the vector $\mathbf{V}^{n+1}$ is calculated as

$$V_i^{n+1}=(1-\omega)V_i^n+\omega\frac{L_i(\mathbf{V}^n)T(V_{i-1}^{n+1})+U_i(\mathbf{V}^n)T(V_{i+1}^n)-D_i(\mathbf{V}^n)\nu(V_i^n)+\eta_i^j}{1+D_i(\mathbf{V}^n)\mu(V_i^n)}, \qquad (17)$$

$$(i=0,\dots,K).$$

In both algorithms, the parameter ω is introduced to improve convergence. We recommend to define this parameter as follows:

$$\omega(E)=\begin{cases}\omega_0, & E<E_-,\\ (1-\omega_0)(E-\rho_S C_S T_{pl})\rho_S^{-1}\lambda^{-1}+\omega_0, & E_-\le E\le E_+,\\ 1, & E_+<E,\end{cases}$$

where ω_0 is an arbitrary parameter (referred to as the accelerating parameter); $1 \le \omega_0 < 2$. In both (16) and (17), ω is calculated by using the values found at the preceding iteration step. In [8, 9] it was proved that the proposed iterative processes are convergent under certain conditions, and various examples of Stefan-type problems solved by applying algorithms (16) and (17) to the corresponding systems of algebraic equations were presented.

Previously, we used both the modified Jacobi algorithm and the modified Gauss-Seidel algorithm to solve problem (13). In the course of our computations, we found that the rate of convergence of the iterative processes (16) and (17) executed to solve the actual systems of algebraic equations was low. It was also found that the iterative processes could be substantially accelerated by using a new procedure [10]. Let us define the vector $\mathbf{V}^{n+1}$ at each iteration step as a solution to the following system of equations:

$$-L_i(\mathbf{V}^n)\mu(V_{i-1}^n)V_{i-1}^{n+1}+[1+D_i(\mathbf{V}^n)\mu(V_i^n)]V_i^{n+1}-U_i(\mathbf{V}^n)\mu(V_{i+1}^n)V_{i+1}^{n+1}=$$

$$= L_i(\mathbf{V}^n)\nu(V_{i-1}^n) - D_i(\mathbf{V}^n)\nu(V_i^n) + U_i(\mathbf{V}^n)\nu(V_{i+1}^n) + \eta_i^j, \qquad (18)$$
$$(i = 0, \ldots, K).$$

System (18) has a tridiagonal matrix. If the time step τ^j is not too large, then this matrix has a diagonal dominance, and system (18) can be solved by means of the efficient tridiagonal algorithm. The new iterative process (18), combined with the tridiagonal algorithm for determining a solution at the $(n+1)$-th iteration step, is the essence of the proposed modification of the approaches developed in [8,9].

The process of solving (13) is terminated by determination of the melting front. Define $E_{pl} = (E_- + E_+)/2$. If the conditions $E_z^j \geq E_{pl}$ and $E_{z+1}^j < E_{pl}$ are satisfied for some $0 \leq z \leq K$ at $t = t^j$, then the melting radius is calculated as

$$\xi^j = \frac{(E_{pl} - E_{z+1}^j)(r_z - r_{z+1})}{E_z^j - E_{z+1}^j} + r_{z+1}. \qquad (19)$$

4 The solution of the variation problem

The variation problem formulated in Chapter 1 was solved numerically by gradient methods . For calculation the gradient of function the Fast Automatic Differentiation methodology was used [11]. To pick comparison functions from the set of class $K(\Theta)$ piecewise continuous functions, we used the method of external penalty functions. In this approach, the set of admissible comparison functions is much broader than $K(\Theta)$, but the cost functional is minimized by an element of the class $K(\Theta)$. This reduces the constraint minimization of the cost functional J in (11) to the unconstraint minimization of the generalized functional $I = J + g(\xi_f) + \Xi$, were $g(r) = A_0(r - R_{pl})^2$ (with a constant A_0) is the penalty functional responsible for the fulfillment of the condition $\xi_f = R_{pl}$, and

$$\Xi = \int_0^\Theta A(t)\left(\frac{d\xi}{dt} + d^2\right)dt, \qquad A(t) = \begin{cases} 0, & \left(\frac{d\xi}{dt} + d^2\right) \geq 0, \\ A_0(t), & \left(\frac{d\xi}{dt} + d^2\right) < 0, \end{cases}$$

is the penalty functional ensuring an admissible cooling rate. Here $\xi_f = \max\limits_{1 \leq j \leq M} \xi^j$, were ξ^j is given by (19). If this maximum is reached at $j = n$ $(1 \leq n \leq M)$, then

$$\xi_f = \frac{(E_{pl} - E_{z+1}^n)(r_z - r_{z+1})}{E_z^n - E_{z+1}^n} + r_{z+1}.$$

Using the rectangles method to approximate the functional J in (11), we obtain the following approximate expression for the generalized functional I:

$$I \approx \tilde{I} = \sum_{j=1}^{M} \tau^j f^j + \tilde{I}^1 + \tilde{I}^2, \quad \tilde{I}^1 = A_0\left[\frac{(E_{pl} - E_{z+1}^n)(r_z - r_{z+1})}{E_z^n - E_{z+1}^n} + r_{z+1} - R_{pl}\right]^2,$$

$$\tilde{I}^2 = \sum_{j=1}^{M} \tau^j A^j(\sigma^j + d^2), \qquad A^j = A(t^j), \qquad \sigma^j = \left(\frac{d\xi}{dt}\right)^j.$$

The Fast Automatic Differentiation methodology allows us to deduce next formula for calculation the components of the gradient of the generalized functional I:

$$\frac{d\tilde{I}}{df^j} = \tau^j + \sum_{i=0}^{w} \tau^j p_i^j \varphi_i, \qquad (1 \le j \le M),$$

were w is the vertex number defined by the condition

$$\varphi(r) = \begin{cases} \varphi_w(r) \neq 0, & 0 \le r \le r_w, \\ 0, & r > r_w. \end{cases}$$

In this expression p_i^j denote the values of conjugate variables (impulses). The impulses are determined by the next linear system of algebraic equations:

$$p_i^{M+1} = 0, \qquad (i = 0, \ldots, K),$$

$$p_0^j = -a_0 Y_1^j p_0^j + b_1 Y_1^j p_1^j + p_0^{j+1} + \tilde{I}^1_{E_0^j} + \tilde{I}^2_{E_0^j},$$

$$p_1^j = a_0 X_1^j p_0^j - a_1 Y_2^j p_1^j - b_1 X_1^j p_1^j + b_2 Y_2^j p_2^j + p_1^{j+1} + \tilde{I}^1_{E_1^j} + \tilde{I}^2_{E_1^j},$$

$$p_i^j = a_{i-1} X_i^j p_{i-1}^j - a_i Y_{i+1}^j p_i^j - b_i X_i^j p_i^j + b_{i+1} Y_{i+1}^j p_{i+1}^j + p_i^{j+1} + \tilde{I}^1_{E_i^j} + \tilde{I}^2_{E_i^j},$$

$$(2 \le i \le K-2),$$

$$p_{K-1}^j = a_{K-2} X_{K-1}^j p_{K-2}^j - b_{K-1} X_{K-1}^j p_{K-1}^j - a_{K-1} Y_K^j p_{K-1}^j + b_K Y_K^j p_K^j +$$

$$+ p_{K-1}^{j+1} + \tilde{I}^1_{E^j_{K-1}} + \tilde{I}^2_{E^j_{K-1}},$$

$$p_K^j = a_{K-1} X_K^j p_{K-1}^j - b_K X_K^j p_K^j - a_K \alpha T'_{E_K^j}(E_K^j) p_K^j + p_K^{j+1} + \tilde{I}^1_{E_K^j} + \tilde{I}^2_{E_K^j},$$

$$(j = M, M-1, \ldots, 1).$$

Here X_i^j and Y_i^j denote the following derivatives:

$$X_i^j = \frac{\partial}{\partial E_i^j}\left(\hat{\Omega}(E_{i-1}^j) T(E_i^j)\right) - \frac{\partial}{\partial E_i^j}\left(\hat{\Omega}(E_{i-1}^j) T(E_{i-1}^j)\right),$$

$$Y_i^j = \frac{\partial}{\partial E_{i-1}^j}\left(\hat{\Omega}(E_{i-1}^j) T(E_{i-1}^j)\right) - \frac{\partial}{\partial E_{i-1}^j}\left(\hat{\Omega}(E_{i-1}^j) T(E_i^j)\right),$$

and $\tilde{I}^1_{E_i^j}$, $\tilde{I}^2_{E_i^j}$ represent the partial derivatives of the functions $\tilde{I}^1$, $\tilde{I}^2$ with respect to E_i^j:

$$\tilde{I}^1_{E_i^j} = \begin{cases} \Lambda(E_{pl} - E^n_{z+1}), & i = z, & j = n, \\ \Lambda(E^n_z - E_{pl}), & i = z+1, & j = n, \\ 0, & & \text{in other case}, \end{cases}$$

$$\tilde{I}^2_{E_i^j} = \sum_{j=1}^{M} \left(A^j \tau^j \frac{\partial \sigma^j}{E_i^j} \right),$$

$$\Lambda = 2A\frac{(r_{z+1}-r_z)}{(E_z^n - E_{z+1}^n)^2}\left[\frac{(E_{pl}-E_{z+1}^n)(r_z-r_{z+1})}{E_z^n - E_{z+1}^n} + r_{z+1} - R_{pl}\right].$$

To find $\tilde{I}^2_{E_i^j}$, we have to evaluate $\partial\sigma^j/\partial E_i^j$. So first we describe an algorithm for determining $\{\sigma^j\}$ (see Fig.2).

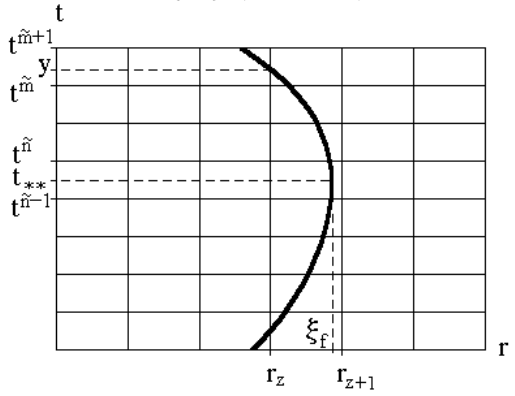

Fig. 2a

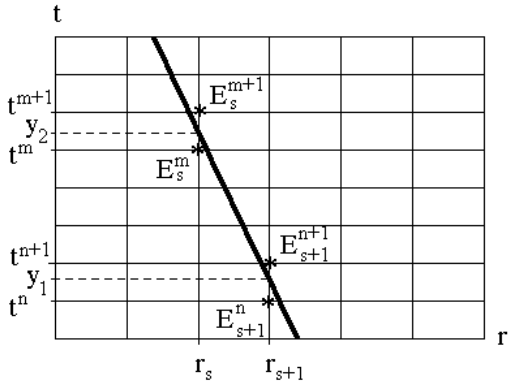

Fig. 2b

Suppose that $r = \xi(t)$, describing interface motion has its maximum value ξ_f at $t = t_{**}$, where ξ_f is defined as

$$\xi_f = \frac{(E_{pl}-E_{z+1}^{\tilde{n}})(r_z-r_{z+1})}{E_z^{\tilde{n}} - E_{z+1}^{\tilde{n}}} + r_{z+1}.$$

Here the index z indicates a spatial interval containing the maximum of $r = \xi(t)$, i. e. $r_z < \xi_f \le r_{z+1}$ (see Fig. 2a), and the index $\tilde{n}$ separates the time intervals before and after $t = t_{**}$, i. e. $t^{\tilde{n}-1} < t_{**} \le t^{\tilde{n}}$. The index $\tilde{m}$ can be used to determine a time interval containing the intersection point (r_z, y) of the curve $r = \xi(t)$ of the coordinate line $r = r_z$, i. e. $t^{\tilde{m}} \le y \le t^{\tilde{m}+1}$. Now all components of $\{\sigma^j\}$ can be divided into two groups: regular and singular. The coordinates of $\{\sigma^j\}$ and their partial derivatives for each group are calculated by somewhat different formulas. While deriving these formulas, we assumed in both cases that the slope of $r = \xi(t)$ (i. e., the component σ^j) within a single spatial cell is a constant and the energy E_i^j is a linear function on $[t^j, t^{j+1}]$.

1. Let us consider the singular group first. It consists of those components of $\{\sigma^j\}$ for which the corresponding $\xi^j = \xi(t^j)$ belong to the interval $r_z < \xi^j \le \xi_f$ or, equivalently, for which $\tilde{n} \le j \le \tilde{m}$ (see Fig. 2a). The component σ^j of $\{\sigma^j\}$ can be calculated by the formula $\sigma^j = (r_z - \xi_f)/(y - t_{**})$. Introducting the notation $b_1^* = E_z^{\tilde{m}+1} - E_z^{\tilde{m}}$, $b_2^* = E_{z+1}^{\tilde{n}} - E_z^{\tilde{n}}$, $\nu^* = (E_{pl} - E_z^{\tilde{m}})\tau^{\tilde{m}+1} + b_1^*(t^{\tilde{m}} - t^{\tilde{n}})$ and taking into account that the time $t = y$ can be found by linear interpolation as

$$y = \frac{(E_{pl} - E_z^{\tilde{m}+1})\tau^{\tilde{m}+1}}{E_z^{\tilde{m}+1} - E_z^{\tilde{m}}} + t^{\tilde{m}+1},$$

we can represent the component σ^j of $\{\sigma^j\}$ as $\sigma^j = h_z b_1^*(E_z^{\tilde{n}} - E_{pl})/b_2^*\nu^*$. Each σ^j depends on the point energy values $E_z^{\tilde{m}}$, $E_z^{\tilde{m}+1}$, $E_z^{\tilde{n}}$, and $E_{z+1}^{\tilde{n}}$. Consequently, the ex-

pression for $\tilde{I}^2_{E_i^j}$ contains the derivatives of σ^jonly with respect to these components of the energy vector. These derivatives are calculated by the formulas:

$$\frac{\partial\sigma^j}{\partial E_z^{\tilde{n}}} = \frac{c_1^*(E_{z+1}^{\tilde{n}} - E_{pl})}{(b_2^*)^2}, \qquad \frac{\partial\sigma^j}{\partial E_{z+1}^{\tilde{n}}} = \frac{c_1^*(E_{pl} - E_z^{\tilde{n}})}{(b_2^*)^2},$$

$$\frac{\partial\sigma^j}{\partial E_z^{\tilde{m}}} = \frac{c_2^*\tau^{\tilde{m}+1}(E_z^{\tilde{m}+1} - E_{pl})}{(\nu^*)^2}, \quad \frac{\partial\sigma^j}{\partial E_z^{\tilde{m}+1}} = \frac{c_2^*\tau^{\tilde{m}+1}(E_{pl} - E_z^{\tilde{m}})}{(\nu^*)^2},$$

where $c_1^* = h_z b_1^*/\nu^*, \quad c_2^* = h_z(E_z^{\tilde{n}} - E_{pl})/b_2^*$.

2. Now consider the regular group of components. It consists of all components of $\{\sigma^j\}$ not included in the singular group. A characteristic feature of this group is that $\xi^j \le r_z$. Suppose that the interface $r = \xi(t)$ intersects the coordinate line $r = r_{s+1}$ at the point $t = y_1$ lying on the time interval $(t^n, t^{n+1}]$ and intersects the coordinate line $r = r_s \quad (r_s < r_{s+1})$ at the point $t = y_2$, $y_2 \in (t^m, t^{m+1}]$ (see Fig.2b). Then all σ^j whose index j satisfies $n < j \le m$ can be calculated by the formula $\sigma^j = (r_s - r_{s+1})/(y_2 - y_1) = h_s/(y_1 - y_2)$. The times $t = y_1$ and $t = y_2$ can be found by linear interpolation:

$$y_1 = \frac{(E_{pl} - E_{s+1}^{n+1})\tau^{n+1}}{E_{s+1}^{n+1} - E_{s+1}^n} + t^{n+1}, \qquad y_2 = \frac{(E_{pl} - E_s^{m+1})\tau^{m+1}}{E_s^{m+1} - E_s^m} + t^{m+1}.$$

As a result, σ^j is expressed as $\sigma^j = a_1^* a_2^* h_s/z^*$, where

$$a_1^* = E_s^{m+1} - E_s^m, \qquad a_2^* = E_{s+1}^{n+1} - E_{s+1}^n,$$

$$z^* = a_1^*(E_{pl} - E_{s+1}^n)\tau^{n+1} - a_2^*(E_{pl} - E_s^m)\tau^{m+1} + a_1^* a_2^*(t^n - t^m).$$

Each σ^j depends on the point energy values E_s^m, E_s^{m+1}, E_{s+1}^{n+1}, and E_{s+1}^n. Consequently, the expression for $\tilde{I}^2_{E_i^j}$ contains the derivatives of σ^j only with respect to these components of the energy vector. These derivatives are calculated by the formulas:

$$\frac{\partial\sigma^j}{\partial E_s^m} = h_s(a_2^*)^2\tau^{m+1}(E_{pl} - E_s^m - a_1^*)/(z^*)^2,$$

$$\frac{\partial\sigma^j}{\partial E_s^{m+1}} = h_s(a_2^*)^2\tau^{m+1}(E_s^m - E_{pl})/(z^*)^2,$$

$$\frac{\partial\sigma^j}{\partial E_{s+1}^n} = h_s(a_1^*)^2\tau^{n+1}(E_{s+1}^n - E_{pl} + a_2^*)/(z^*)^2,$$

$$\frac{\partial\sigma^j}{\partial E_{s+1}^{n+1}} = h_s(a_1^*)^2\tau^{n+1}(E_{pl} - E_{s+1}^n)/(z^*)^2.$$

In the other cases, $\partial\sigma^j/\partial E_i^j$ was set equal to zero.

5 The results of solution of variation problem

The variation problem, with the input parameters varying in wide ranges, was solved numerically in numerous runs. The qualitative behavior of the optimal control of melting and solidification and its structure were found to depend weakly on the input parameters of the problem.

All results presented below were obtained for the following thermophysical parameters given in SI units:

$$\rho_S = 7700, \quad k_S = 22, \quad C_S = 730, \quad \rho_L = 7700, \quad k_L = 22,$$

$$C_L = 730, \quad T_{pl} = 1773.15, \quad T_{ex} = 293.15, \quad T_{in}(r) \equiv 293.15,$$

$$\alpha = 1, \quad \lambda = 1291666.615.$$

Previously, the equations and the boundary conditions were nondimensionalized. Changing to dimensionless variables, we divided all the lengths by R_{pl}; all the temperatures by T_{pl}; the density, heat conductivity, and specific heat capacity by their respective means ρ_*, k_*, and C_*; the time by $R_{pl}^2\rho_* C_*/k_*$; and the source strength F by $k_* T_{pl}/R_{pl}^2$. In what follows, all the quantities are dimensionless.

The computations were performed on a nonuniform spatial grid containing 400 nodes. The grid was finer toward the axis $r = 0$ and the line $r = R_{pl}$. The time step was constant and was chosen so as to ensure the required accuracy of numerical results. The source was nearly a point ($r_w = 0.003$).

An analysis of the numerical results obtained suggests the following conclusions about the structure of the optimal control:

(i) The optimal control consists of two basic components.

(ii) The first optimal-control component (responsible primarily for melting) coincides with the upper bound $f(t) \equiv f_{max}$.

(iii) The second optimal-control component (responsible for solidification) is smaller than the first (if we compare their averages) and is separated from the latter by a short interval with $f(t) \equiv 0$.

(iv) The time t_{on} for which the source is turned on at the phase of solidification depends on both f_{max} and the limit cooling rate d^2. Depending on these parameters, t_{on} either precedes the time t_{**} at which the extent of the melted domain reaches its maximum possible value $\xi(t_{**}) = R_{pl}$ (for small values of d^2), succeeds t_{**} (for large values of d^2), or coincides with it.

To illustrate the general structure of the optimal control, Fig.3 shows its temporal dependencies obtained by solving the variation problem. The plots correspond to $f_{max} = 10.0$ and $d^2 = 0.3$ (Fig.3a), $f_{max} = 10.0$ and $d^2 = 0.4$ (Fig.3b), and $f_{max} = 5.0$ and $d^2 = 0.5$ (Fig.3c).

In the article the influence of different parameters of the problem on to optimal control was investigated.

a) Influence of d^2 on the First Optimal-Control Component

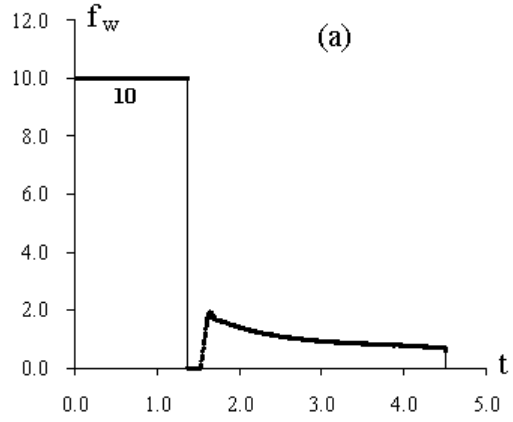

Fig. 3a

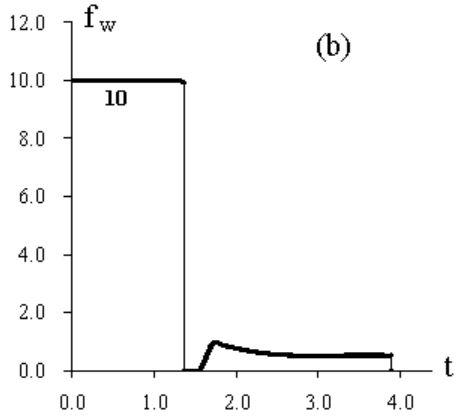

Fig. 3b

In all the regimes, the first optimal-control component is given by

$$f_{opt}(t) = \begin{cases} f_{max}, & 0 \le t \le t_*, \\ 0, & t_* < t. \end{cases} \tag{20}$$

Here, t_* (the time for which the source is turned on at the melting stage) depends on the regime.

If d^2 is such that $t_{on} \ge t_{**}$, then t_* is determined by the condition that the maximum radius of the melted domain is R_{pl} for the source defined by (20); i.e. $\xi_f = R_{pl}$. In this case, the first optimal-control component is not affected by the second one.

If d^2 is such that $t_{on} < t_{**}$, then the first optimal-control component is affected by the second. The value of t_* somewhat decreases in this case. However, our numerical computations have shown that this effect is small and can be neglected within the accuracy of the numerical results.

Hence, the first optimal-control component can be determined regardless of the second component by applying the algorithm described in [12].

b) Influence of d^2 on the Second Optimal-Control Component

We examined how the second optimal-control component depends on d^2 for a fixed f_{max}. Both the first and the second optimal-control components were determined by solving the variation problem. Figure 4 shows the optimal distributions of the source strength f_w vs. time for various values of d^2. The number near a curve indicates the value of d^2 used for obtaining this optimal control. An analysis of the numerical results presented in Fig. 4a,b,c shows that the optimal controls corresponding to different values of d^2 behave likewise, and all characteristic parameters (the length of the interval $t \in [t_{**}, \Theta_* - \beta^2]$, the maximum and minimum values of $f_w(t)$, etc.) decrease with increasing d^2 (for details see [13]).

c) Influence of f_{max} on the Second Optimal-Control Component

We also examined how the second optimal-control component depends on f_{max} for a fixed d^2. The numerical computations revealed that f_{max} has a large effect on

the second optimal-control component. Figure 5 displays the location of the liquid — solid interface vs. time. The source was defined by (20) at the stage of melting and was not turned on at the stage of solidification (which corresponds to $d^2 = \infty$). The digits near the curves indicate the value of f_{max} used in the determination of the corresponding front. The value of R_{pl} is reached more rapidly when f_{max} is higher. The segments of the curves corresponding to the motion of the solidification front seem parallel, but this is not the case. For smaller values of f_{max}, the trajectory is steeper and the solidification rate is lower. Inspection of the plots suggests that small values of f_{max} are preferable. However, numerous computations have shown that it is preferable to increase f_{max}, thus increasing the violation of (10) and, accordingly,

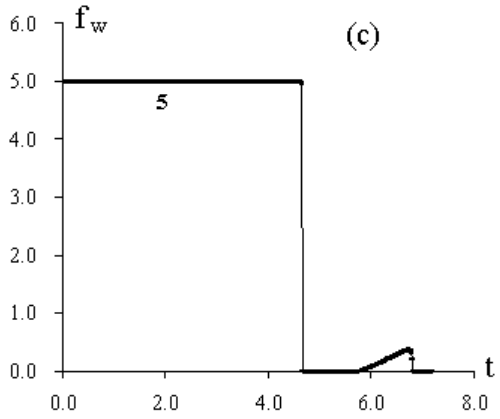

Fig. 3c

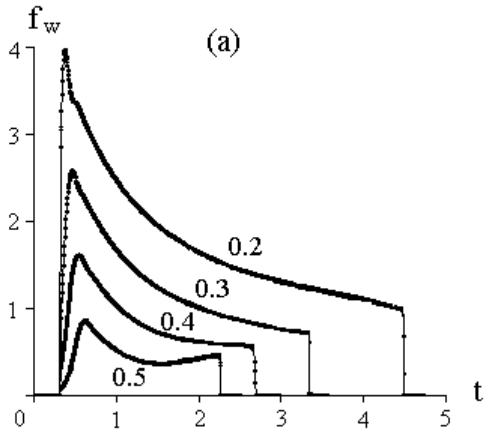

Fig. 4a

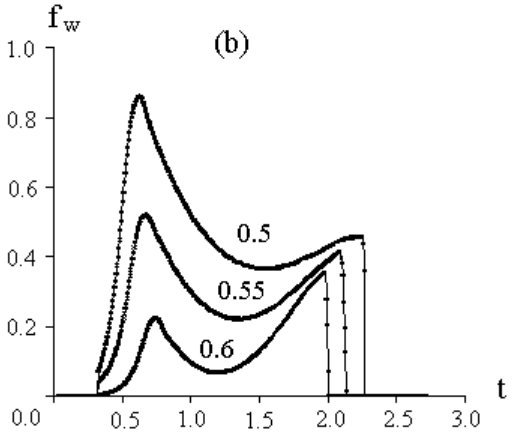

Fig. 4b

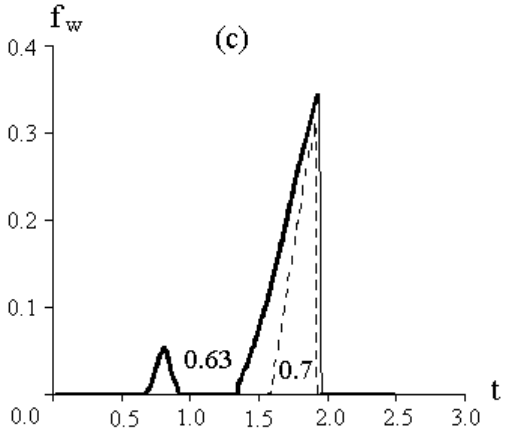

Fig. 4c

increasing the source strength at the solidification stage.

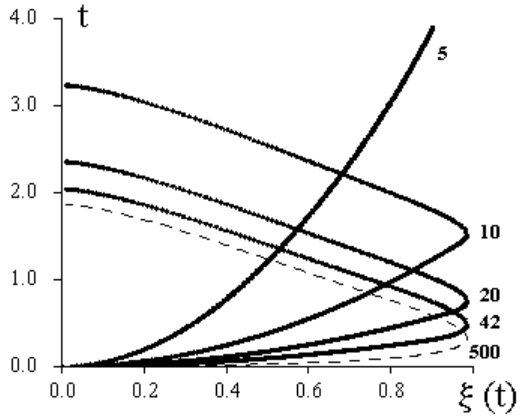

Fig. 5

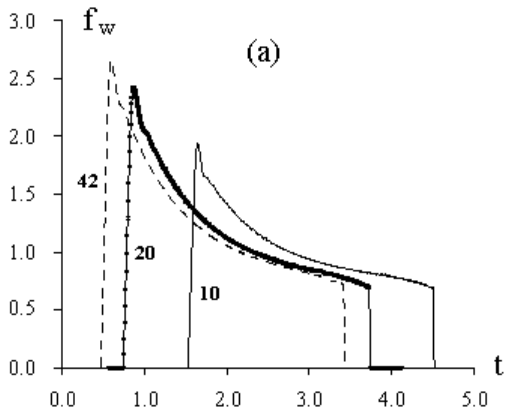

Fig. 6a

To confirm this conclusion, the full variation problem was solved numerically with $f_{max} = 9.98$ and $f_{max} = 10.0$. The resulting values of the cost functional were found to be $J_w = 15.160$ and $J_w = 15.152$, respectively. Figure 6 shows the optimal control at the stage of solidification (the second optimal-control component) for various values of f_{max}. Figures 6a and 6b correspond to $d^2 = 0.3$, and Figs.6c and 6d, to $d^2 = 0.4$. The digits near the curves indicate the corresponding values of f_{max}. The zero time corresponds to the beginning of the process. It should be noted that the second optimal-control components qualitatively resemble each other for various parameter values. The larger the value of f_{max}, the earlier is the turn-on time at the stage of solidification. The smaller the value of d^2, the higher the source strength at the respective instants and the longer the turn-on time. It should be noted that the second optimal-control components approach each other as f_{max} increases. The curves for which $f_{max} > 80.0$ are virtually indistinguishable. The functional values virtually do not differ from those corresponding to $f_{max} = 500$ (see Table 1).

d) Influence of f_{max} and d^2 on the Functional

To determine the effect of these parameters on the optimal control, we carried out a large amount of computations. Some of the results are presented in the Table 1, which lists the values of J_w, $J_w^{(1)}$, and $J_w^{(2)}$. As mentioned above, the heat source was turned on twice: at the stage of melting and at the stage of solidification. The regimes under study were chosen so that the time intervals with the source turned on were not overlapped. In this case, J_w in (12) can be represented as the sum $J_w = J_w^{(1)} + J_w^{(2)}$, where $J_w^{(1)}$ is the heat supplied during the first turn-on (melting) and $J_w^{(2)}$ is the heat supplied during the second turn-on (solidification). Based on numerous numerical results, the following conclusions can be made about the influence of f_{max} and d^2 on the cost functional value corresponding to the optimal control (see Table 1).

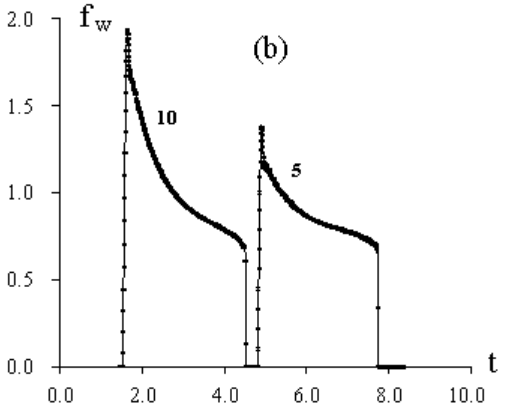

Fig. 6b

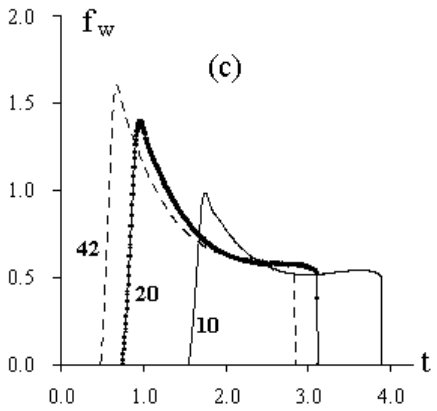

Fig. 6c

(i) The larger f_{max}, the smaller the values of J_w and $J_w^{(1)}$.

(ii) The larger d^2, the smaller the values of J_w and $J_w^{(2)}$.

(iii) The larger f_{max}, the larger the value of $J_w^{(2)}$.

(iv) The contribution of $J_w^{(2)}$ to J_w (the ratio $J_w^{(2)}/J_w^{(1)}$) increases with f_{max}.

These conclusions are supported by the plots of J_w, $J_w^{(1)}$, and $J_w^{(2)}$ vs. f_{max} for $d^2 = 0.4$ displayed in Fig. 7. Note that the qualitative behavior of J_w and $J_w^{(1)}$ is similar.

Importantly, the smaller d^2, the greater the number of iterations and CPU time required for obtaining the optimal control, although qualitative changes in the optimal control vs. time were not observed. For small values of d^2, small variations in this parameter lead to substantial quantitative changes in the optimal control. For example, for $f_{max} = 10$, we have $\max f_w(t) \approx 1$ for $d^2 = 0.4$, $\max f_w(t) \approx 2$ for $d^2 = 0.3$, and $\max f_w(t) \approx 4$ for $d^2 = 0.2$. a similar dependence is observed for the duration ΔT of the source operation: $\Delta T \approx 2.3$ for $d^2 = 0.4$, $\Delta T \approx 3.0$ for $d^2 = 0.3$, and $\Delta T \approx 4.5$ for $d^2 = 0.2$.

Note that the contribution of $J_w^{(2)}$ to J_w is not small and increases noticeably with decreasing d^2 for a fixed f_{max}. For example, at $f_{max} = 10$, we have $J_w^{(2)}/J_w \approx 0.03$ for $d^2 = 0.5$, $J_w^{(2)}/J_w \approx 0.09$ for $d^2 = 0.4$, $J_w^{(2)}/J_w \approx 0.18$ for $d^2 = 0.3$, and $J_w^{(2)}/J_w \approx 0.32$ for $d^2 = 0.2$ (see Table 1).

e) Alongside with the problem posed above two supplementary subproblems were studied: the problem of melting at absence of limitations (10) on speed of crystallization [12] and task of crystallization at given control at a stage of melting [13].

The first part of optimal control (responsible for melting process) has next structure [12] . If there were no restrictions on source power from top then the optimal control represents the injection all necessary heat at initial time moment; if there are restrictions from the top then the optimal control consists of two parts coincide

Table 1

f_{max}		5	10	20	42	500
d^2						
0.5	J_w	23.4906	14.2022	12.0533	11.3994	11.1772
	$J_w^{(1)}$	23.2843	13.7659	11.3264	10.5337	10.2544
	$J_w^{(2)}$	0.2063	0.4363	0.7269	0.8657	0.9228
0.4	J_w	24.2699	15.1520	13.0855	12.4537	12.2483
	$J_w^{(1)}$	23.2841	13.7630	11.3264	10.5337	10.2507
	$J_w^{(2)}$	0.9858	1.3890	1.7591	1.9200	1.9976
0.3	J_w	25.8284	16.8314	14.8389	14.2136	14.0131
	$J_w^{(1)}$	23.2850	13.7659	11.3260	10.5336	10.2540
	$J_w^{(2)}$	2.5434	3.0655	3.5129	3.6800	3.7591
0.2	J_w		20.2064			
	$J_w^{(1)}$		13.7640			
	$J_w^{(2)}$		6.4424			

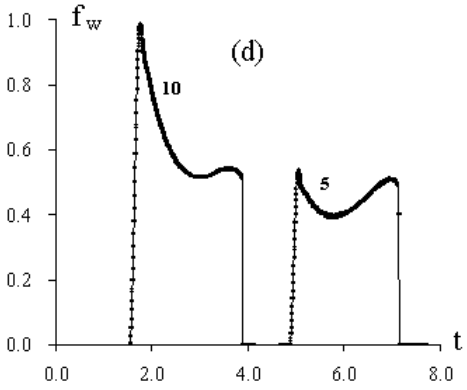

Fig. 6d

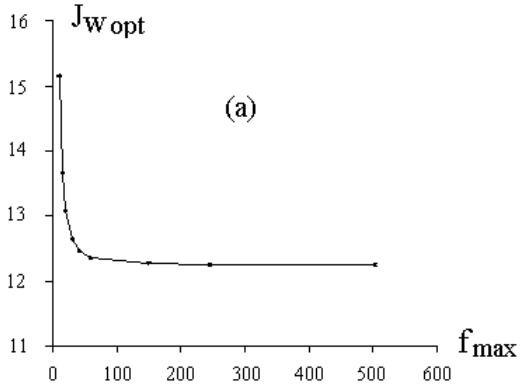

Fig. 7a

with the boundary. If the heat source is distributed in space the structure of optimal control is the same.

As the optimal control at a stage of melting coincides the upper boundary restriction, for its determination it is necessary to find only moment of switchover of a source from the upper limitation on lower.

The optimal control on the stage of substance crystallization consists also of two parts [13] . First, it coincides with lower boundary of the source power constraint and then changes over (continuously or stepwise) to the second part. This second

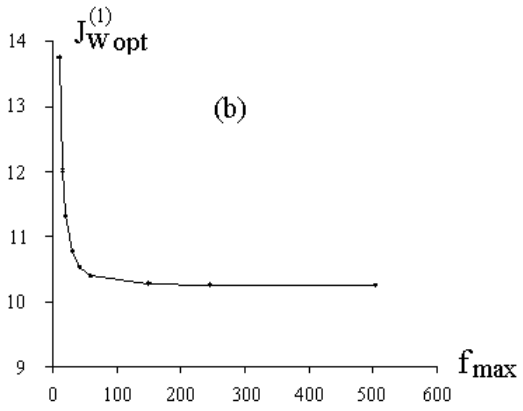

Fig. 7b

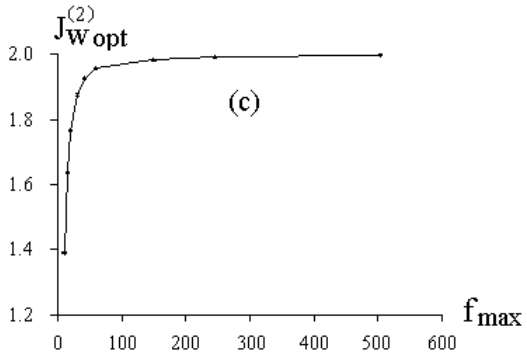

Fig. 7c

part is determined by requirements that the rate of the crystallization front should be not more than given amount and that emerged energy of the source should be minimal.

The numerous results of the solution of the supplementary problems have coincided with large accuracy with the applicable results, which one were obtained at the solution of the problem in full posing. It is no wonder: as is marked in post a), with accuracy of spent calculations the first part of optimal control is instituted irrespective of the second part.

The investigations of the problem permit to make following conclusions. In the parameter range that was used while investigations took part, the optimal control could be determined from the solution of two successive problems. First, we solve the melting problem and then, using its results as the initial data for the second one, we examine the crystallization problem. Usage of such splitting at the solution of the full variation problem essentially economizes expenditures on deriving of the optimal solution.

References

[1] Lions J.-L. *Controle optimal de systemes gouvernes par des equations au derivees partielles*. Paris, Gauthier-Villars, 1968; Moscow, Mir, 1972.

[2] Lur'e K.A. *Optimal Control in Problems of Mathematical Physics*. Moscow, Nauka, 1975 (in Russian).

[3] Ahmed N.U., Teo K.L. *Optimal Control of Distributed Parameter Systems*. New York, North Holland, 1981.

[4] Vasil'ev F.P. *Optimization Methods*. Moscow, Faktorial, 2002 (in Russian).

[5] Yurii A.D. *An Optimal Stefan-Type Problem*. Dokl. Akad. Nauk SSSR, 1980, **251**, p. 1317–1321.

[6] Gol'dman N.L. *Inverse Stefan Problems: Theory and Solution Methods*. Moscow, Mosk. Gos. Univ., 1999 (in Russian).

[7] Rose M.E. *A Method for Calculating Solutions of Parabolic Equations with a Free Boundary*. Math. Comput., 1960, **14**, p. 249–256.

[8] White R.E. *An Enthalpy Formulation of the Stephan Problem*. SIAM J. Numer. Anal., 1982, **19**, p. 1129–1157.

[9] White R.E. *A Numerical Solution of the Enthalpy Formulation of the Stephan Problem*. SIAM J. Numer. Anal., 1982, **19**, p. 1158–1172.

[10] Albu A.F., Zubov V.I. *Modified Scheme for Analyzing the Process of Melting*. Zh. Vychisl. Mat. Mat. Fiz., 2001, **41**, p. 1434–1443 (Comp. Math. Math. Phys., 2001, **41**, p. 1363–1371).

[11] Evtushenko Y.G. *Computation of Exact Gradients in Distributed Dynamic Systems*. Optimizat. Methods and Software, 1998, **9**, p. 45–75.

[12] Albu A.F., Gorbunov V.I., Zubov V.I. *Optimal Control of the Process of Melting*. Zh. Vychisl. Mat. Mat. Fiz., 2000, **40**, p. 517–531 (Comp. Math. Math. Phys., 2000, **40**, p. 491–504).

[13] Albu A.F., Zubov V.I. *Optimal Control of the Process of Solidification*. Zh. Vychisl. Mat. Mat. Fiz., 2004, **44**, p. 38–50 (Comp. Math. Math. Phys., 2004, **44**, p. 34–44).

V.I. Zubov
Computing Centre of Russian Academy of Sciences
GSP-1, 117967, Moscow, Russia
E-mail: *zubov@ccas.ru*

Received December 9, 2004